
Epistemic Neural Networks

Ian Osband, Zheng Wen, Mohammad Asghari,
Morteza Ibrahimi, Xiyuan Lu, and Benjamin Van Roy

DeepMind

{iosband,zhengwen,smasghari,mibrahimi,lxlu,benvanroy}@deepmind.com

Abstract

We introduce the *epistemic neural network* (ENN) as an interface for uncertainty modeling in deep learning. All existing approaches to uncertainty modeling can be expressed as ENNs, and any ENN can be identified with a Bayesian neural network. However, this new perspective provides several promising directions for future research. Where prior work has developed probabilistic inference tools for neural networks; we ask instead, ‘which neural networks are suitable as tools for probabilistic inference?’. We propose a clear and simple metric for progress in ENNs: the KL-divergence with respect to a target distribution. We develop a computational testbed based on inference in a neural network Gaussian process and release our code as a benchmark at <https://github.com/deepmind/enn>. We evaluate several canonical approaches to uncertainty modeling in deep learning, and find they vary greatly in their performance. We provide insight to the sensitivity of these results and show that our metric is highly correlated with performance in sequential decision problems. Finally, we provide indications that new ENN architectures can improve performance in both the statistical quality and computational cost.

1 Introduction

The only admissible decision rules are Bayesian (Wald, 1992). This means that if you have a decision rule that is not Bayesian, you can improve the statistical quality of its decisions with a Bayesian alternative (Cox and Hinkley, 1979). An important caveat is that for large and complex problems, the computational requirements of exact Bayesian inference can quickly become intractable (Andrieu et al., 2003). Deep learning methods have emerged as the state of the art method across many fields of artificial intelligence, with statistical flexibility and computational scalability suitable for large and complex problems (Krizhevsky et al., 2012; Devlin et al., 2019). However, the majority of deep learning systems completely neglect *epistemic*¹ uncertainty, the key component of Bayesian decision making. This paper seeks to reconcile this disconnect.

The majority of deep learning research has evolved outside of Bayesian, and sometimes even statistical analysis (LeCun et al., 2015); nevertheless, there is a long and persistent history of research in Bayesian neural networks (BNNs) (Neal, 2012). This research has contributed both new methods that can quantify epistemic uncertainty (Blundell et al., 2015), as well as new perspectives on existing methods that aim to deepen our statistical understanding of deep learning (Mandt et al., 2018). Research in this area is experiencing a resurgence of interest from a wide variety of perspectives, but it can be difficult to tell exactly what progress is being made. Different strands in the literature use different notation

¹*Epistemic* uncertainty relates to knowledge (ancient Greek *episteme* ↔ knowledge), as opposed to *aleatoric* uncertainty relating to chance (Latin *alea* ↔ dice) (Kendall and Gal, 2017).

and benchmark problems, with subtle differences in the actual problems they are trying to solve. This means it can be difficult to understand the progress in the field and even agree where popular methods perform well or poorly (Osband, 2016; Hron et al., 2017). Further, despite this wealth of research, and the pressing need for uncertainty quantification in real systems, most large-scale applications of deep learning do not provide uncertainty estimates (Gal, 2016). Effective uncertainty estimates may be crucial for safe and fair AI (Mitchell et al., 2019). We believe that this paper can help to drive this field forward by clarifying the interface and problem formulation for uncertainty estimation in neural networks.

Bayesian deep learning has mostly focused on the challenge of developing tools for probabilistic inference in neural networks. In this paper, we pose the mirror challenge of developing neural networks for probabilistic inference. To this end, we introduce the *epistemic neural network* (ENN) as an interface for uncertainty modeling in deep learning. Further, we propose the KL divergence from a target distribution as a precise metric for the quality of an ENN. We describe this interface formally in Section 2, but provide a high level summary of the approach here. For any input $x \in \mathcal{X}$, an ENN f makes prediction $f_\theta(x, z)$ based on its parameters $\theta \in \Theta$ and an *epistemic index* $z \in \mathcal{Z}$. An ENN also specifies a reference distribution P_Z such that the resultant $f_\theta(x, z)|_{z \sim P_Z}$ produces a predictive distribution for the ENN. ENNs are mathematically equivalent to BNNs; but the ENN formulation offers a valuable new perspective to the field. We assess the *quality* of an ENN through the statistical divergence between the resulting ENN distribution and a target posterior. The goal of research then becomes to develop approaches that have high statistical quality in posterior approximation, but that can scale computationally to large and complex problems better than exact Bayesian inference. Our results in Section 4 provide clear and reproducible rankings for posterior approximation, which can help to clarify when/where competing approaches to uncertainty quantification perform well (Ovadia et al., 2019).

Our next major contribution is to develop a computational testbed to assess ENN quality in a computationally efficient manner. We package these tools in software which we release in supplementary material (see Appendix A). Section 3 describes the methodology for this testbed, but we provide a high level summary of the approach here. We specify a target posterior in terms of the neural network Gaussian process (NNGP) obtained in the limit of infinite width. We use the *neural tangents* library to compute the target NNGP posterior (Novak et al., 2020), and a sample-based approximation to estimate the KL divergence of ENN predictions. We validate the empirical convergence of these estimates and provide optimized, user-friendly code using Jax for the research community (Bradbury et al., 2018).

One key aspect of this testbed is that it is based on a *generative model* for the underlying posterior inference, rather than a finite set of benchmark datasets (LeCun et al., 1998). As such, it is inoculated against some of the dangers of overfitting to any particular dataset. Even where researchers might tune myriad parameters for each problem instance, a generative model can always provide new streams of testing data. The testbed provides a simple and sanitized problem, where we can objectively talk about the ‘correct’ answer with full control over problem definitions. This is an important contribution to the field, which we outline in Section 3.1. It is important to note that this generative testbed is complementary to, and not a replacement for, benchmark performance on real datasets or challenge problems. Further, we show in Section 4.3 that performance on our testbed is correlated with performance in sequential decision problems.

On one level, epistemic neural networks are simply a notational convenience: any existing deep learning procedure can be written as an ENN, and rewriting an existing method as an ENN will not improve its performance. However, we believe this simplicity hides deeper insights that makes the ENN perspective worthwhile. First, adopting this common language facilitates clearer thinking and comparison across different-but-related approaches to posterior approximation. Then, armed with this unifying perspective, the problem of developing a better ENN becomes a problem of designing better loss functions, optimization algorithms or network architecture. Section 4.2 shows that we can use these insights to develop new ENN architectures that match existing state of the art statistical quality, but at orders of magnitude less compute. We believe that the ENN perspective, coupled with the testbed for ENN evaluation, will open up exciting new avenues of research and help to accelerate our progress towards effective uncertainty estimates in large and complex systems.

2 Epistemic Neural Networks

This section presents two of the main contributions of the paper; the ENN interface, and a problem formulation for approximate posterior inference using neural networks. All existing approaches to uncertainty modeling in deep learning can already be expressed as ENNs. ENNs present a new perspective for thinking about neural networks as computational tools for approximate posterior inference.

2.1 An interface for epistemic uncertainty in deep learning

A ‘vanilla’ neural network takes an input $x \in \mathcal{X}$, parameters $\theta \in \Theta$ and makes predictions $f_\theta(x)$ without explicit regard for epistemic uncertainty. Bayesian neural networks (BNNs) augment this formulation to consider a *distribution* over plausible parameters $\theta \sim \phi$. Where ϕ corresponds to the posterior distribution updated by Bayes’ rule, the resultant distribution of predictions $f_\theta(x)|_{\theta \sim \phi}$ represents the posterior predictive distribution for the BNN. The grand challenge of Bayesian deep learning is to develop effective tools for probabilistic inference, and therefore uncertainty estimates, where f is a deep neural network.

In this paper, we present a mirrored challenge: to develop neural networks that are effective tools for probabilistic inference. To this end, we define an *epistemic* neural network (ENN) that takes an input $x \in \mathcal{X}$, parameters $\theta \in \Theta$ and an *epistemic index* $z \in \mathcal{Z}$ to make a prediction $f_\theta(x, z)$. An ENN also specifies a reference distribution P_Z such that the distribution of $f_\theta(x, z)|_{z \sim P_Z}$ represents the predictive distribution of the ENN. Figure 1 provides a graphical illustration of these different network formulations. At a high level, ENNs are designed to take the complex problem of posterior inference in BNNs, which normally occurs *outside* of the network architecture, and instead allow the network to learn the posterior distribution via the epistemic index *input* to the network.

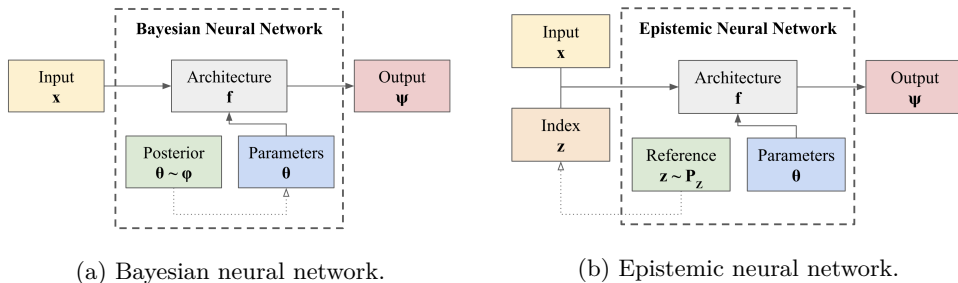


Figure 1: Comparing network paradigms. Dotted arrows indicate that sampling (a) parameters or (b) indices from this distribution can produce an approximate posterior distribution.

2.2 Probabilistic Inference via Neural Networks

Along with the ENN interface, we develop a problem formulation and a clear metric for ENN performance. At a high level, we assess the statistical quality of an ENN through the quality of the posterior approximation it provides in terms of KL divergence from a *target* posterior (Kullback and Leibler, 1951). Of course, this quantity can be minimized by the target posterior itself, but we are motivated by large, complex environments where exact Bayesian computation is intractable. Depending on the setting, useful ENNs should also consider computational constraints in both training and evaluation in order to provide genuine value. This style of evaluation via generative model, rather than challenge datasets, is somewhat unusual among deep learning research but we provide justification for why this constitutes an essential addition to the community in Section 3.1.

In this paper we consider a simple regression problem $y_{t+1} = f^*(x_t) + \epsilon_{t+1}$, for $x_t \sim P_X$ and $\epsilon_{t+1} \sim P_E$ both sampled i.i.d. We leave a more general investigation of learning, including classification, to future work. Let $\mathbb{P}(f^* \in \cdot)$ denote the prior over the underlying function f^* . In this setting, the distribution over f^* specifies the epistemic uncertainty, while the addition of ϵ_{t+1} adds an element of aleatoric uncertainty to the distribution of y_{t+1} . For

any dataset $\mathcal{D}_T = \{(x_t, y_{t+1}) \text{ for } t = 0, \dots, T-1\}$, we can write $\mathbb{P}(f^*(X) \in \cdot | \mathcal{D}_T, X)$ for the posterior of f^* given \mathcal{D}_T , evaluated at X . Compared to this idealized target posterior, we consider the performance of an **EnnAgent**, which maps training data \mathcal{D}_T , and a random draw to parameters θ_T for an ENN f . We define the *average* KL divergence

$$\bar{\mathbf{d}}_{\text{KL}} := \mathbb{E}[\mathbf{d}_{\text{KL}}(\mathbb{P}(f^*(X) \in \cdot | \mathcal{D}_T, X) \| \mathbb{P}(f_{\theta_T}(X, z \sim P_Z) \in \cdot | \theta_T, X))], \quad (1)$$

where the expectation is taken over the input data X , the training data \mathcal{D}_T and the random draw in **EnnAgent** generating θ_T . This metric matches ‘negative log-likelihood’ on a test dataset common to the literature, in the case where predictions are made without aleatoric uncertainty. Section 3.2 provides more details on the choice of prior $\mathbb{P}(f^* \in \cdot)$ that we focus on in this paper. Section 3.3 outlines the mathematical and computational tools we develop to estimate $\bar{\mathbf{d}}_{\text{KL}}$ effectively.

We argue that $\bar{\mathbf{d}}_{\text{KL}}$ is also of fundamental interest to sequential decision problems. Imagine a decision maker that selects action $x_t \in \mathcal{X}$, in order to maximize utility y_{t+1} in an uncertain environment. The realized utility can be expressed as a combination of expected value $f^*(x_t) = \mathbb{E}[y_{t+1} | x_t]$ and chance $\epsilon_{t+1} = y_{t+1} - f^*(x_t)$. An **EnnAgent** that performs well according to $\bar{\mathbf{d}}_{\text{KL}}$, on average, produces an ENN predictive distribution that is close to the true posterior distribution evaluated at an input X and so, might usefully drive decision making in this context. In Section 4.3, we present an empirical evaluation that performance in (1) is strongly correlated with performance in sequential decision problems.

2.3 Where might ENNs add value?

Figure 1 a direct equivalence between ENNs and BNNs: any ENN can be expressed as a BNN, and any BNN can be expressed as an ENN. To see this, note that in any ENN we can relate the parameters θ and index $z \sim P_z$ as augmented parameters $\tilde{\theta} := (\theta, z)$ in a BNN with appropriately matched posterior $\tilde{\phi}$. Rewriting any method as an ENN will not change the quality of its posterior approximation; as such, there is a sense that ENNs are nothing more than a new notation for existing concepts. However, we believe that this simple observation hides a deeper truth: that ENN perspective make particular architectures and losses become more natural than in the BNN framing.

Neural networks and stochastic gradient descent have emerged as key tools for statistical learning in complex, high-dimensional problems. These successes have, for the most part, run ahead of the theoretical foundations of deep learning (Zhang et al., 2017). This poses a great challenge to BNNs: given a neural network procedure that produces effective point estimates, how can we apply approximate posterior inference to obtain a full posterior distribution. Here the ‘unreasonable effectiveness’ of deep learning provides an impediment to progress. ENNs aim to turn the power of neural networks towards posterior inference. Where a BNN’s posterior distribution ϕ exists outside the network parameters; in ENNs, the parameters θ encode the full knowledge distribution. As such, the ENN perspective suggests novel network architectures designed to perform approximate Bayesian inference, beyond MAP estimates (Dutordoir et al., 2021). In Section 4.2, we show that novel architectures can match existing statistical quality at orders of magnitude less computation.

We also believe that the problem formulation (1) will be valuable for clarity and progress in the field. Where BNNs are assessed purely on challenge problems, there are several distinct questions at play. Whether or not a BNN performs well *in a given task* is a distinct question from whether the BNN approximates the true Bayesian posterior well, or even if the Bayesian posterior is a suitable model for this problem (Izmailov et al., 2021). As we outline in Section 3.1, this type of evaluation is prone to overfitting, and makes iterative progress difficult. Since ENN performance is explicitly evaluated in terms of divergence from a target distribution, we can clearly evaluate the settings and metrics in which one technique is preferable to another. Section 4 compares performance of four benchmark approaches, and allows a scientific comparison of approaches in a like-for-like manner. A major limitation of this metric however, is that it requires access to a high-quality approximation of the posterior $\mathbb{P}(f^* \in \cdot | \mathcal{D}_T)$. As such, it may be unsuitable at present for use in ‘cutting edge’ AI applications such as large language models without further work (Brown et al., 2020). We recognize that this paper only begins to make progress in such research, but we believe that the ENN perspective will help to accelerate progress in this area.

3 Gaussian Process Testbed

This section presents our next major contribution in this paper: a practical testbed for comparing the quality of ENNs according to $\bar{\mathbf{d}}_{\text{KL}}$. We will first make a clear case for why the field needs a generative testbed to supplement the many dataset-based challenges for uncertainty estimation. Next, we will describe the particular choice of generative model that we will focus on in this paper. Finally, we will outline the mathematical methods and contributions that allow us to estimate $\bar{\mathbf{d}}_{\text{KL}}$ efficiently in this setting.

3.1 Why do we need a testbed with synthetic data?

A key property of the testbed is that it is specified by a probabilistic model, rather than a finite collection of datasets. Benchmarks that rank performance on datasets are vulnerable to overfitting through iterative hill-climbing on the data included in the benchmark (Russo and Zou, 2016), which may not generalize to data outside of the benchmark (Recht et al., 2018). In contrast, access to a generative model means that we can produce an unlimited amount of testing data from our problem of interest. With access to this generative model, we can avoid the dangers of overfitting to any specific choices of benchmark dataset simply by generating more samples.

Another benefit of studying ENN quality in problems with synthetic data is that it provides a simple problem which we can fully understand. This sanitized setting allows us the ability for precise scientific experiments, and easily varying model conditions (kernel, dataset size T , input dimension $D_{\mathcal{X}}$ etc.) and to investigate their effects. Real-world problems remain an important benchmark for measuring progress; synthetic problems can be a valuable complement to understand that progress. In problems where we have access to an underlying generative model, we can use this to provide principled, accurate and practical methods to compute the quality of an ENN relative to the target posterior.

3.2 Neural network Gaussian processes

Our problem formulation in Section 2.2 suggests that it does not make sense to talk about a ‘good’ ENN, unless you can define the generative model you are trying to approximate. In this paper we focus on a specific generative model for f^* described by an NNGP (Lee et al., 2018). We write κ^1 for the kernel derived from the limit of an infinitely-wide neural network, with two hidden layers and ‘ReLU’ activation function. The weights in each layer $l = 0, 1, 2$ and the biases in layer $l = 0$ are initialized according to $N(0, 1/n_l)$; and the biases in layer $l = 1, 2$ are fixed to 0. Note that $n_0 = D_{\mathcal{X}}$ is the dimension of the input x , and we take the limit $n_1, n_2 \rightarrow \infty$ for infinite width. To evaluate the quality of the ENNs across a variety of settings, we generate 10 random seeds for each of input dimensions $D_{\mathcal{X}} \in \{1, 10, 100\}$, number of training datapoints $T = \lambda D_{\mathcal{X}}$ for data ratio $\lambda \in \{1, 10, 100\}$ and noise standard deviation $\sigma \in \{0.01, 0.1, 1\}$. We fix $P_X = N(0, I)$.

We have chosen to focus our attention on this kernel for a few reasons. Principally, we choose a specific kernel for the sake of clarity in a short paper. Most of the tools and techniques we develop would apply to *any* valid probabilistic model, but by picking a particular kernel we make it easier to understand the general approach. Further, we do believe this kernel is fundamentally interesting to deep learning problems for a few reasons; the GP limit of wide neural networks can describe the behaviour of finite networks (de G. Matthews et al., 2018), learning with this kernel can perform well on simple deep learning benchmarks (Lee et al., 2018), and this kernel passes basic ‘sanity checks’ on its data requirements. Finally, our results in Section 4.1 show that ranking on κ^1 is highly correlated with ranking on other NNGP kernels (varying depth and activation function) so we know these results are somewhat robust. We provide more details on all of these justifications in Appendix C.

3.3 Evaluating ENN quality

We now describe the computational approach to KL estimation. At a high level, we use a finite sample-based approach to approximate the expectations in $\bar{\mathbf{d}}_{\text{KL}}$. Concretely, we first sample T training inputs x_0, \dots, x_{T-1} and T' cached testing inputs $x_T, \dots, x_{T+T'-1}$

i.i.d. from $P_X = N(0, I)$. Next, we sample a function f^* from a given GP prior $N(\mu, \kappa)$ (e.g. $N(0, \kappa^1)$), restricted to the training inputs and cached testing inputs. We generate the training outputs as $y_{t+1} = f^*(x_t) + \epsilon_{t+1}$, where ϵ_{t+1} is independently sampled from $N(0, \sigma^2)$. The training dataset is $\mathcal{D}_T = \{(x_t, y_{t+1}) \text{ for } t = 0, \dots, T-1\}$.

We use \mathcal{D}_T to train an ENN f_{θ_T} , and compute the Gaussian posterior $N(\bar{\mu}, \bar{\kappa})$ over the cached testing inputs based on Bayes' rule. Then for each $n = 1, \dots, N$, we sample $x^{(n)}$ uniformly randomly from the cached inputs, and use $\bar{\mu}^{(n)}$ and $\bar{\kappa}^{(n)}$ to respectively denote the marginal posterior mean and variance at $x^{(n)}$. We sample M epistemic indices $z_1^{(n)}, \dots, z_M^{(n)}$ i.i.d. from the ENN's reference distribution P_Z , and use $\hat{\mu}^{(n)}$ and $\hat{\kappa}^{(n)}$ to respectively denote the sample mean and variance of $f_{\theta_T}(x^{(n)}, z_1^{(n)}), f_{\theta_T}(x^{(n)}, z_2^{(n)}), \dots, f_{\theta_T}(x^{(n)}, z_M^{(n)})$. We can then estimate,

$$\begin{aligned} \mathbb{E}[\mathbf{d}_{\text{KL}}(\mathbb{P}(f^*(X) \in \cdot | \mathcal{D}_T, X) \| \mathbb{P}(f_{\theta_T}(X, z \sim P_Z) \in \cdot | \mathcal{D}_T, X)) | \mathcal{D}_T, \theta_T] \\ \approx \frac{1}{N} \sum_{n=1}^N \mathbf{d}_{\text{KL}}(N(\bar{\mu}^{(n)}, \bar{\kappa}^{(n)}) \| N(\hat{\mu}^{(n)}, \hat{\kappa}^{(n)})). \end{aligned} \quad (2)$$

Finally, we introduce multiple random seeds to average $\bar{\mathbf{d}}_{\text{KL}}$ over training data \mathcal{D}_T and trained parameters θ_T . We provide a detailed pseudo-code for the entire procedure in Appendix B, together with empirical validation that these estimates are within required statistical tolerance for our ranking at the selected values $T' = N = 1000, M = 100$.

4 Results

In this section we present the main experimental results of this paper. We begin with a large-scale evaluation of several benchmark approaches to uncertainty estimation in neural networks. Our results provide clear evidence that these methods can differ wildly in their statistical quality according to $\bar{\mathbf{d}}_{\text{KL}}$. We provide some insight to the sensitivity of these results across problem settings, and show these findings are extremely robust to changes in NNGP kernel. Next, we illustrate the potential benefits that can arise from effective ENN network design: presenting a novel distillation approach to *learn* an uncertainty estimate that reduces computational inference cost by over an order of magnitude. Finally, we present an investigation of the same ENN agents applied to a sequential decision problem. We find that performance on the GP testbed is highly correlated with performance of a sequential decision agent that employs that ENN for approximate posterior inference.

4.1 Testbed ranking

We evaluate several benchmark approaches to uncertainty estimation in deep learning, applied to our testbed from Section 3.2.² We provide full implementations details, including code, in Appendix A. We base all agents around a 50-50-MLP architecture trained by Adam with learning rate 10^{-3} over 1k minibatches of size 100.³

- **dropout**: dropout rate 0.05, weight regularization 10^{-6} (Gal and Ghahramani, 2016).
- **bbb**: (Bayes by backprop) prior weight variance $\sigma_0^2 = 10^4$ (Blundell et al., 2015).
- **hypermodel**: linear hypermodel with index dimension 20, additive prior function and additive Gaussian noise in learning targets per Dwaracherla et al. (2020).
- **ensemble**: with 30 elements, each with additive prior functions and additive Gaussian noise in the learning targets per Osband et al. (2018).

In each case, we attempted to match the ‘canonical’ implementation outlined in the cited papers and chose under-specified parameters via grid search. Figure 2 shows the overall breakdown in score over the testbed.

²Infinitely wide 2-layer ReLU NNGP κ^1 , estimate $\bar{\mathbf{d}}_{\text{KL}}$ (1) over 10 random seeds for each of `input_dim`= $D_X \in \{1, 10, 100\}$, `data_ratio`= $\lambda \in \{1, 10, 100\}$ and `noise_std`= $\sigma \in \{0.01, 0.1, 1\}$.

³We ran all experiments on an internal CPU cluster in parallel. In total, the main agents' results requires around 100 CPU-hours and the full parameter sweeps close to 10K CPU-hours.

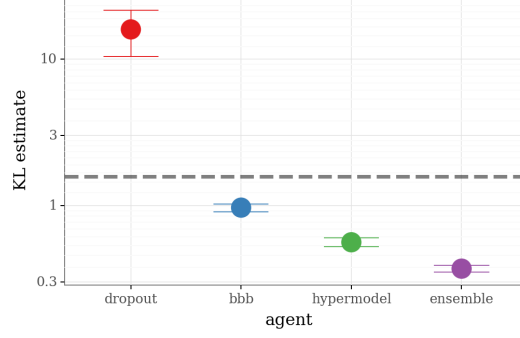


Figure 2: Testbed scores vary significantly for benchmark agents, lower is better. Error bars at $\pm 1\text{stderr}$. Dashed line indicates the $\bar{\mathbf{d}}_{\text{KL}}$ of an uninformed baseline $N(0, 1)$ prediction.

These results present several statistically significant findings. Dropout performs extremely poorly according to our testbed metric, with average scores 10x worse than an uninformed $N(0, 1)$ prediction in this setting. The best performing agent overall is the ensemble with additive prior functions and additive target noise. Bootstrapping, or data perturbation, is crucial to performance on our testbed and we provide more details on this observation in Appendix A.4 (Nixon et al., 2020). However, this *overall* metric is an average over many different problem instances. Figure 3 provides more insight by looking into the average $\bar{\mathbf{d}}_{\text{KL}}$ as we vary each of `data_ratio`= λ , `input_dim`= $D_{\mathcal{X}}$ and `noise_std`= σ .

Examining the effects of `data_ratio`= λ , we see most agents are relatively stable in their ranking, apart from dropout. We note that, as λ increases dropout not only outperforms the uninformed baseline, but also improves on BBB. Examining the effects of `input_dim`= $D_{\mathcal{X}}$ shows that both BBB and hypermodel tend to improve as we increase dimension. We hypothesize this is due to difficulties in optimizing their loss functions in the low dimension (and thus less convex) loss landscape. Finally, looking at `noise_std`= σ we see that ensembles greatly outperform other approaches in the low noise regime, but that both hypermodel and BBB are competitive in high noise environments.

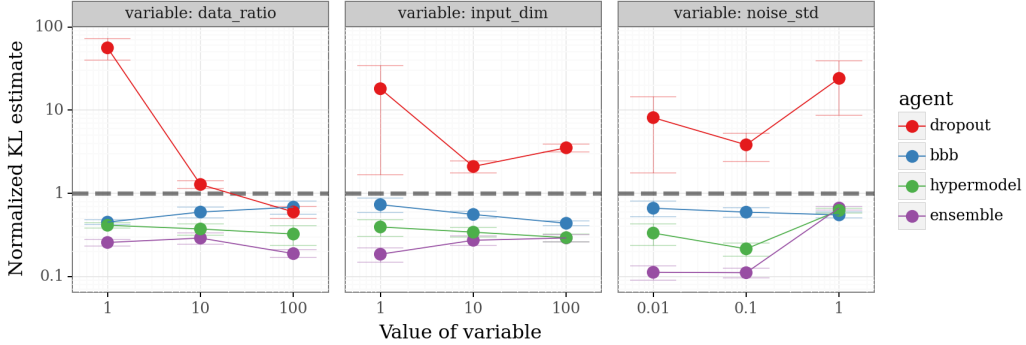


Figure 3: Sensitivity of $\bar{\mathbf{d}}_{\text{KL}}$ when restricting (`data_ratio`, `input_dim`, `noise_std`).

Our testbed results focus on the kernel κ^1 defined in Section 3.2 as a 2-layer ReLU NNGP. One concern might be that observations for this kernel do not carry over to other posterior inference challenges. Figure 4 shows the relation of our testbed metric to that calculated under alternative NNGPs with layers $L = 1, 2, 3$ and both Erf and ReLU activations. In each case these results are highly correlated, pointing to the robustness of our testbed evaluation.

Although we have only presented these results for simple/benchmark agents, we believe that these observations may prove valuable to the community and encourage more researchers to compare their approaches. We believe that these results may help to reconcile several outstanding questions in the field. In the next subsection, we take some of the first steps towards novel ENN design, and show the potential for orders of magnitude savings in computation.

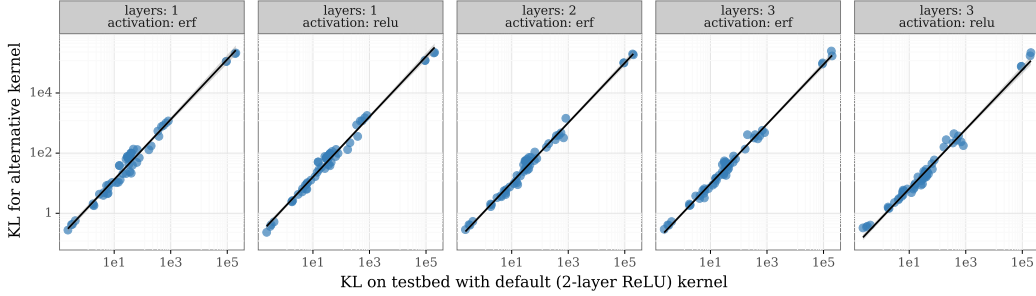


Figure 4: Estimates of $\bar{\mathbf{d}}_{\text{KL}}$ under alternative kernels are all highly correlated (> 0.98).

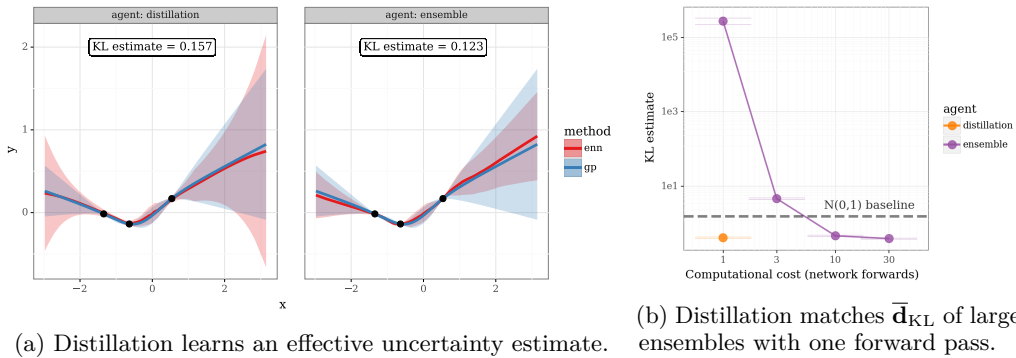
4.2 ENNs can offer orders of magnitude savings in computation

Our results in Section 4.1 reaffirm the general effectiveness of ensembles (with suitable prior functions and bootstrapping) to generate high quality posterior samples in neural networks. However, this high *statistical* quality can come at a significant computational cost. In an ensemble, each element is learned independently and hence, the computational costs grow linearly in the number of elements. Other ENN architectures such as dropout, BBB or hypermodel share parameters across epistemic indices, so that (at least in theory) they might benefit from generalization across $z \in \mathcal{Z}$. However, for many applications, the computational cost at *test* inference can present a prohibitive cost. In each of the ENNs of Section 4.3 generating a posterior sample costs one full network forward. Generating reasonable uncertainty estimates may require orders of magnitude more computation than a single MAP estimate, which might not be practical for deployment in a real-world setting. In this section, we present a stylized ENN network architecture that shows it is possible to save orders of magnitude improvements in computational costs at test time.

We introduce a novel agent based around ensemble *distillation* (Hinton et al., 2015). For an ensemble of size K , we train a $(K + 1)$ -th particle to output $(\hat{\mu}, \log(\hat{\sigma}^2))$ of the first K predictions. To do this, we periodically sample a ‘fake batch’ $\hat{x} \sim P_X$ and optimize the $(K + 1)$ -th particle via KL-divergence on a matched Gaussian. Write $\hat{\mu} := \frac{1}{K} \sum_{k=1}^K f_k(x)$ and $\hat{\sigma}^2(x) := \frac{1}{K-1} \sum_{k=1}^K (f_k(x) - \hat{\mu})^2$ then we define the loss evaluated at x ,

$$\mathcal{L}(x) := \frac{1}{2} \left(\log \left(\frac{\hat{\sigma}^2}{\tilde{\sigma}^2} \right) + \frac{\hat{\sigma}^2}{\tilde{\sigma}^2} + \frac{(\hat{\mu} - \tilde{\mu})^2}{\tilde{\sigma}^2} - 1 \right). \quad (3)$$

We outline full details of this approach, including code, in Appendix A. Figure 5a shows that a distillation agent can effectively generalize uncertainty estimates of an ensemble. Figure 5b shows that a distillation agent can, on average, match performance in $\bar{\mathbf{d}}_{\text{KL}}$ of an ensemble $K = 30$ with only one network forward.



(a) Distillation learns an effective uncertainty estimate.

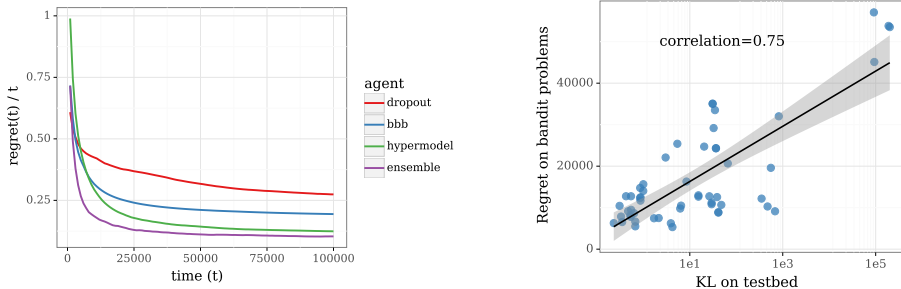
(b) Distillation matches $\bar{\mathbf{d}}_{\text{KL}}$ of larger ensembles with one forward pass.

Figure 5: Training an ENN via distillation effectively amortizes computation in training for reduced costs at test inference. This is a simple ‘proof of concept’ for more exotic ENNs.

4.3 Relation to sequential decision problems

In Section 2.2, we suggest that our testbed metric is partially motivated by sequential decision problems; we now provide an empirical evaluation relating ENN performance in these settings. To do this, we introduce a class of GP bandit problems derived from our testbed formulation (Gittins, 1979). We then evaluate the performance of a *Thompson sampling* (TS) agent, varying only the ENN used for posterior approximation (Thompson, 1933). A TS agent maintains a posterior distribution of beliefs and, at each timestep, selects an action randomly according to the posterior probability it is the optimal action (Russo et al., 2018). This simple heuristic can effectively balance the needs of exploration and exploitation, and allows us to evaluate the ability of an approximate ENN posterior to drive decision making. Our results show that performance on the testbed is highly correlated with performance in the sequential decision problem.

To form a GP bandit given prior $N(\mu, \kappa)$ and input distribution P_X , we first sample actions $\mathcal{A} = \{a^1, \dots, a^A\}$ i.i.d. from P_X and a function $f^* \sim N(\mu, \kappa)$. At each timestep t an agent selects action $a_t \in \mathcal{A}$, and receives reward $r_{t+1} = f^*(a_t) + \epsilon_{t+1}$, for $\epsilon_{t+1} \sim N(0, \sigma^2)$ i.i.d. We assess agent performance through the $\text{regret}(T) := \sum_{t=0}^{T-1} \mathbb{E}[\max_a f^*(a) - f^*(a_t)]$, which measures the shortfall in expected cumulative rewards relative to an optimal decision maker. At each timestep t , our TS agent updates its ENN f_{θ_t} based on past observations; it then samples index $z_t \sim P_Z$ and selects action $a_t \in \arg \max_{a \in \mathcal{A}} f_{\theta_t}(a, z_t)$. We provide full implementation details and code in Appendix A. Figure 6a shows the average regret through time of our testbed agents applied to a bandit problem derived from κ^1 with $D_X = 10$, $A = 10D_X$ and $\sigma^2 = 0.01$. Figure 6b shows the average relationship between performance on the testbed and a matched sweep over bandit problems ($D_X \in \{1, 10, 100\}$, $\sigma \in \{0.01, 0.1, 1\}$, each with 10 seeds) after 100,000 steps. The general pattern is clear, performing better on our testbed leads, on average, to better performance in sequential decision problems.



(a) Agents applied to a GP bandit.

(b) Performance is correlated with testbed.

Figure 6: Relating the testbed performance to sequential decision problems.

5 Conclusion

ENNs present an interface for uncertainty modeling that flips some elements of Bayesian deep learning on its head. Rather than research probabilistic inference tools for neural networks, we ask which neural networks are suitable tools for probabilistic inference. We are excited to release mathematical and computational tools that allow researchers to clearly rank performance of ENNs in relation to a target posterior. Our results show that, in our testbed, dropout performs poorly as an ENN, suitably-bootstrapped ensembles can perform remarkably well while linear hypermodels and BBB lie somewhere in between. Our work is preliminary, in that we focus on a simple and sanitized problem of NNGP regression. Even so, we show that these metrics are robust to the choice of kernel, and correlated with performance in sequential decision problems. Our ‘distillation’ ENN also provides a simple ‘proof of concept’ that innovations in ENN design may offer orders of magnitude improvements in statistical quality and/or computational cost. We hope that this paper will provide a foundation for more exciting work in this direction.

References

- Andrieu, C., De Freitas, N., Doucet, A., and Jordan, M. I. (2003). An introduction to mcmc for machine learning. *Machine learning*, 50(1):5–43.
- Blundell, C., Cornebise, J., Kavukcuoglu, K., and Wierstra, D. (2015). Weight uncertainty in neural network. In *International Conference on Machine Learning*, pages 1613–1622. PMLR.
- Bradbury, J., Frostig, R., Hawkins, P., Johnson, M. J., Leary, C., Maclaurin, D., Necula, G., Paszke, A., VanderPlas, J., Wanderman-Milne, S., and Zhang, Q. (2018). JAX: composable transformations of Python+NumPy programs.
- Brown, T. B., Mann, B., Ryder, N., Subbiah, M., Kaplan, J., Dhariwal, P., Neelakantan, A., Shyam, P., Sastry, G., Askell, A., et al. (2020). Language models are few-shot learners. *arXiv preprint arXiv:2005.14165*.
- Cox, D. R. and Hinkley, D. V. (1979). *Theoretical statistics*. CRC Press.
- de G. Matthews, A. G., Rowland, M., Hron, J., Turner, R. E., and Ghahramani, Z. (2018). Gaussian process behaviour in wide deep neural networks.
- Devlin, J., Chang, M.-W., Lee, K., and Toutanova, K. (2019). BERT: Pre-training of deep bidirectional transformers for language understanding. In *Proceedings of the 2019 Conference of the North American Chapter of the Association for Computational Linguistics: Human Language Technologies, Volume 1 (Long and Short Papers)*, pages 4171–4186, Minneapolis, Minnesota. Association for Computational Linguistics.
- Dutordoir, V., Hensman, J., van der Wilk, M., Ek, C. H., Ghahramani, Z., and Durrande, N. (2021). Deep neural networks as point estimates for deep gaussian processes. *arXiv preprint arXiv:2105.04504*.
- Dwaracherla, V., Lu, X., Ibrahimi, M., Osband, I., Wen, Z., and Roy, B. V. (2020). Hypermodels for exploration. In *International Conference on Learning Representations*.
- Gal, Y. (2016). *Uncertainty in Deep Learning*. PhD thesis, University of Cambridge.
- Gal, Y. and Ghahramani, Z. (2016). Dropout as a Bayesian approximation: Representing model uncertainty in deep learning. In *International Conference on Machine Learning*.
- Gittins, J. C. (1979). Bandit processes and dynamic allocation indices. *Journal of the Royal Statistical Society: Series B (Methodological)*, 41(2):148–164.
- Hinton, G., Vinyals, O., and Dean, J. (2015). Distilling the knowledge in a neural network. *arXiv preprint arXiv:1503.02531*.
- Hron, J., Matthews, A. G. d. G., and Ghahramani, Z. (2017). Variational gaussian dropout is not bayesian. *arXiv preprint arXiv:1711.02989*.
- Izmailov, P., Vikram, S., Hoffman, M. D., and Wilson, A. G. (2021). What are bayesian neural network posteriors really like? *arXiv preprint arXiv:2104.14421*.
- Kendall, A. and Gal, Y. (2017). What uncertainties do we need in bayesian deep learning for computer vision? In *Advances in Neural Information Processing Systems*, volume 30.
- Kingma, D. and Ba, J. (2015). Adam: A Method for Stochastic Optimization. *Proceedings of the International Conference on Learning Representations*.
- Krizhevsky, A., Sutskever, I., and Hinton, G. E. (2012). Imagenet classification with deep convolutional neural networks. In *Advances in Neural Information Processing Systems 25*, pages 1097–1105.
- Kullback, S. and Leibler, R. A. (1951). On information and sufficiency. *The annals of mathematical statistics*, 22(1):79–86.
- Lakshminarayanan, B., Pritzel, A., and Blundell, C. (2017). Simple and scalable predictive uncertainty estimation using deep ensembles. In *Advances in Neural Information Processing Systems*, pages 6405–6416.
- LeCun, Y., Bengio, Y., and Hinton, G. (2015). Deep learning. *Nature*, 521(7553):436.

- LeCun, Y., Bottou, L., Bengio, Y., Haffner, P., et al. (1998). Gradient-based learning applied to document recognition. *Proceedings of the IEEE*, 86(11):2278–2324.
- Lee, J., Bahri, Y., Novak, R., Schoenholz, S. S., Pennington, J., and Sohl-Dickstein, J. (2018). Deep neural networks as gaussian processes. In *6th International Conference on Learning Representations, ICLR 2018*.
- Mandt, S., Hoffman, M. D., and Blei, D. M. (2018). Stochastic gradient descent as approximate bayesian inference.
- Mitchell, M., Wu, S., Zaldivar, A., Barnes, P., Vasserman, L., Hutchinson, B., Spitzer, E., Raji, I. D., and Gebru, T. (2019). Model cards for model reporting. In *Proceedings of the conference on fairness, accountability, and transparency*, pages 220–229.
- Neal, R. M. (2012). *Bayesian learning for neural networks*, volume 118. Springer Science & Business Media.
- Nixon, J., Lakshminarayanan, B., and Tran, D. (2020). Why are bootstrapped deep ensembles not better? In *"I Can't Believe It's Not Better!" NeurIPS 2020 workshop*.
- Novak, R., Xiao, L., Hron, J., Lee, J., Alemi, A. A., Sohl-Dickstein, J., and Schoenholz, S. S. (2020). Neural tangents: Fast and easy infinite neural networks in python. In *International Conference on Learning Representations*.
- Osband, I. (2016). Risk versus uncertainty in deep learning: Bayes, bootstrap and the dangers of dropout. In *NIPS Workshop on Bayesian Deep Learning*, volume 192.
- Osband, I., Aslanides, J., and Cassirer, A. (2018). Randomized prior functions for deep reinforcement learning. In Bengio, S., Wallach, H., Larochelle, H., Grauman, K., Cesa-Bianchi, N., and Garnett, R., editors, *Advances in Neural Information Processing Systems 31*, pages 8617–8629. Curran Associates, Inc.
- Osband, I. and Van Roy, B. (2015). Bootstrapped Thompson sampling and deep exploration. *arXiv preprint arXiv:1507.00300*.
- Ovadia, Y., Fertig, E., Ren, J., Nado, Z., Sculley, D., Nowozin, S., Dillon, J. V., Lakshminarayanan, B., and Snoek, J. (2019). Can you trust your model’s uncertainty? evaluating predictive uncertainty under dataset shift. *arXiv preprint arXiv:1906.02530*.
- Recht, B., Roelofs, R., Schmidt, L., and Shankar, V. (2018). Do cifar-10 classifiers generalize to cifar-10? *arXiv preprint arXiv:1806.00451*.
- Russo, D. and Zou, J. (2016). Controlling bias in adaptive data analysis using information theory. In *Artificial Intelligence and Statistics*, pages 1232–1240. PMLR.
- Russo, D. J., Van Roy, B., Kazerouni, A., Osband, I., and Wen, Z. (2018). A tutorial on thompson sampling. *Found. Trends Mach. Learn.*, 11(1):1–96.
- Thompson, W. R. (1933). On the likelihood that one unknown probability exceeds another in view of the evidence of two samples. *Biometrika*, 25(3/4):285–294.
- Wald, A. (1992). Statistical decision functions. In *Breakthroughs in Statistics*, pages 342–357. Springer.
- Zhang, C., Bengio, S., Hardt, M., Recht, B., and Vinyals, O. (2017). Understanding deep learning requires rethinking generalization. In *5th International Conference on Learning Representations, ICLR 2017, Toulon, France, April 24-26, 2017, Conference Track Proceedings*.

Symbol	Explanation	Symbol	Explanation
x	input	\mathcal{X}	input domain
y	output	\mathcal{Y}	output domain
θ	NN parameters	Θ	parameter space
z	epistemic index	\mathcal{Z}	epistemic index space
f	network architecture	\mathcal{D}_T	training data
$D_{\mathcal{X}}$	input dimension	$D_{\mathcal{Z}}$	epistemic index dimension
P_X	input distribution	P_Z	reference distribution
T	# of training data	T'	# of cached testing data
σ	noise standard deviation	M	# of random indices in ENN
N	# of MC simulations in testbed	L	# of hidden layers in NN
μ	mean function of GP	κ	kernel function of GP

Table 1: Reference notation used in the paper.

A Testbed agents

In this section, we describe the implementation of the ENN agents. We pay particular to the five main agents we discuss in Section 4: dropout, bbb, hypermodel, ensemble and distillation. In each case, we aim to provide a simple and minimalist experimental evaluation. Where possible, we follow the implementation of prior work up to the selection of hyperparameters which we tune via grid search. In addition to this appendix, we open-source complete implementation of these **EnnAgents**, and suggest that motivated practitioners consult <https://github.com/deepmind/enn> for full details.

A.1 Dropout

We follow Gal and Ghahramani (2016) to build a dropout agent for posterior approximation. Viewed as an ENN the epistemic index z specifies the bernoulli mask applied to network components. In each iteration, a minibatch $\tilde{\mathcal{D}}$ is sampled uniformly with replacement from training \mathcal{D}_T , and the loss function of the dropout agent is

$$\mathcal{L}(\theta, \tilde{\mathcal{D}}, z) = \frac{1}{|\tilde{\mathcal{D}}|} \sum_{(x,y) \in \tilde{\mathcal{D}}} (y - f_{\theta}(x, z))^2 + \lambda \|\theta\|_2^2,$$

where $\lambda = \frac{\ell^2(1-p_{\text{dropout}})}{2T}$. Here ℓ is length-scale, p_{dropout} is the dropping probability, and T is the number of training data pairs.

We train the network with batch size 32 over 1,000 training steps and Adam optimizer with learning rate 1e-3 (Kingma and Ba, 2015). We perform a grid search over:

- **dropout rate** $p = [0.01, 0.05, 0.1, 0.2, 0.5]$.
- **length scale** $\ell = [0, 1\text{e-}6, 1\text{e-}4, 1\text{e-}2]$.

We select $p = 0.05, \ell = 1\text{e-}6$ by grid search over the testbed, optimizing for $\overline{\mathbf{d}}_{\text{KL}}$. Even with this optimization the overall performance is still even worse than an uniformed agent that predicts $N(0, 1)$.

A.2 Hypermodel

A *hypermodel* is a special case of ENN, for which we have $f_{\theta}(x, z) = f'_{g_{\nu}(z)}(x)$, where f' is the *base model*, g is the *hypermodel*, ν encodes the parameters of the hypermodel, z is the epistemic index, and x is the input. To specify the loss function we form an augmented dataset $\mathcal{D}'_T = \{(x_t, \zeta_t, y_{t+1}), t = 0, \dots, T-1\}$ from \mathcal{D}_T . Following Dwaracherla et al. (2020), ζ_t 's are sampled i.i.d. from P_{ζ} (uniform over the unit hypersphere with dimension $D_{\mathcal{Z}}$). In

each iteration, we sample a minibatch $\tilde{\mathcal{D}}$ from \mathcal{D}'_T , and a set $\tilde{\mathcal{Z}}$ of indices i.i.d. from P_Z . We can then define the loss,

$$\mathcal{L}(\nu, \tilde{\mathcal{D}}, \tilde{\mathcal{Z}}) = \frac{1}{|\tilde{\mathcal{D}}|} \frac{1}{|\tilde{\mathcal{Z}}|} \sum_{z \in \tilde{\mathcal{Z}}} \sum_{(x, \zeta, y) \in \tilde{\mathcal{D}}} (y + \eta \sigma \zeta^T z - f'_{g_\nu(z)}(x))^2, \quad (4)$$

where $\sigma > 0$ is the noise standard deviation, $\eta > 0$ is the noise scale, σ_P^2 is the prior variance, and ν_0 encodes the initial hypermodel parameters.

We train the linear hypermodel $g_\nu(z) = c + Bz$ with batch size 32 over 1,000 training steps of the Adam optimizer with learning rate 1e-3. The hypermodel is initialized based on the Glorot initialization, and a matched additive ‘prior function’, whose output we rescale by $\lambda > 0$ as an additional hyperparameter (Osband et al., 2018). We perform a grid search over:

- **index dimension** $D_Z = [5, 10, 20]$.
- **noise scale** $\eta = [0, 1]$ for use in Equation (4).
- **prior scale** $\lambda = [0, 1, 5]$.

We select $D_Z = 20, \eta = 1, \lambda = 5$ by grid search over the testbed, optimizing for $\bar{\mathbf{d}}_{\text{KL}}$.

A.3 Bayes by backprop

We follow Blundell et al. (2015) to build a Bayes by Backprop (BBB) agent. This agent is based on a diagonal linear hypermodel $f'_{g_\nu(z)}(x)$ where $g_\nu(z) = Bz + c$ and B is a diagonal matrix. We assume that the prior in the parameter space is $N(0, \sigma_0^2 I)$, and the reference distribution P_Z is also $N(0, \sigma_0^2 I)$. Note that $\nu = (B, c)$ specifies a Gaussian distribution in the parameter space, denoted by $P(\theta|\nu)$.

In each iteration, a minibatch $\tilde{\mathcal{D}}$ is sampled uniformly with replacement from the training data \mathcal{D}_T , and a set $\tilde{\mathcal{Z}}$ of indices is sampled i.i.d. from P_Z . The loss function for the BBB agent is a sample-based approximation of the negative evidence lower bound (NELBO):

$$\mathcal{L}(\nu, \tilde{\mathcal{D}}, \tilde{\mathcal{Z}}) = \underbrace{\mathbf{d}_{\text{KL}}(P(\theta|\nu) \parallel N(0, \sigma_0^2 I))}_{\text{complexity cost}} + \underbrace{\frac{1}{2\sigma^2} \frac{T}{|\tilde{\mathcal{D}}|} \frac{1}{|\tilde{\mathcal{Z}}|} \sum_{z \in \tilde{\mathcal{Z}}} \sum_{(x, y) \in \tilde{\mathcal{D}}} (y - f'_{g_\nu(z)}(x))^2}_{\text{negative log-likelihood}}.$$

We train the network with batch size 32 over 1,000 training steps and Adam optimizer with learning rate 1e-3. We perform a grid search over:

- **prior std** $\sigma_0 = [0.1, 0.3, 1, 3, 10, 30, 100]$.

We select $\sigma_0 = 100$ by grid search over the testbed, optimizing for $\bar{\mathbf{d}}_{\text{KL}}$.

A.4 Ensemble

We follow the previous work of Osband et al. (2018) to train an ensemble of networks with matching prior functions and gaussian perturbations to the learning targets. As discussed in Section 2.2 of Dwaracherla et al. (2020), the ensemble agent can be viewed as a special case of hypermodel agents with $g_\nu(z) = \nu z$, where z is a one-hot vector and ν is a matrix encoding the parameters of all models in the ensemble.

We did perform a grid search over hyperparameters. However, unlike the previous sections, this was purely to assess robustness of the solution and ablate factors. The top performing ensemble (size=30, additive prior, additive gaussian noise) applied to 50-50-MLP precisely matches the recommendations in Osband et al. (2018). We train for 1,000 training steps, batch size 32 and adam optimizer learning rate 1e-3.

Figure 7 shows the performance of the ensemble agent as we ablate additive Gaussian noise (noise_scale=0,1) and additive prior function (prior_scale=0,1). We can see that additive target noise (bootstrapping) is absolutely crucial to good performance as an ENN as

those agents with `noise_scale=0` perform poorly overall. Prior functions are also helpful for performance, although this effect is less pronounced overall. Figure 8 shows the sensitivity of these changes in each subset of the testbed settings. As expected, the effects of bootstrap noise are essential in the high noise, low data regime. This may help to settle some of the questions raised by Nixon et al. (2020). Although ‘deep ensembles’ are a popular benchmark approach to uncertainty in deep learning, we show once again that the prior effects can be absolutely crucial (Osband and Van Roy, 2015; Lakshminarayanan et al., 2017).

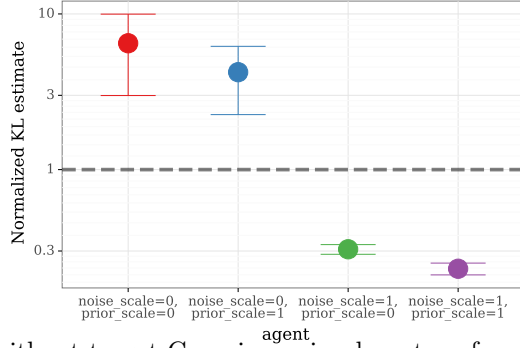


Figure 7: Ensembles without target Gaussian noise do not perform well across the testbed. Prior networks are also helpful in improving performance.

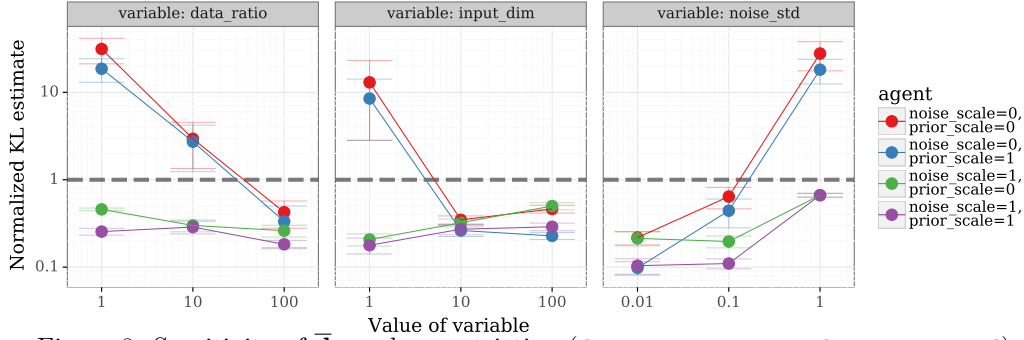


Figure 8: Sensitivity of \bar{d}_{KL} when restricting (`data_ratio`, `input_dim`, `noise_std`).

A.5 Distillation

For the ‘distillation’ agent we augment the ensemble from Section A.4 with two extra 50-50-MLPs that predict $(\tilde{\mu}, \log(\tilde{\sigma}^2))$ per Section 4.2. We train this network in conjunction with the ensemble over 1,000 training steps keeping all settings unchanged from the vanilla ensemble. At test inference the agent forwards only the *distillation* MLPs to obtain the mean and variance estimates.

A.6 Thompson sampling agent

At each timestep t , our TS agent updates its ENN f_{θ_t} based on past observations; it then samples index $z_t \sim P_Z$ and selects action $a_t \in \arg \max_{a \in \mathcal{A}} f_{\theta_t}(a, z_t)$. We perform learning updates according to the appropriate loss function for each ENN outlined above. Each timestep, the agent takes one SGD step using a batch comprised of the most recent 8 observations (a_t, r_{t+1}) . We use ADAM optimizer with learning rate 10^{-3} .

B Gaussian process testbed design

This appendix outlines the details of our GP testbed implementation. First we outline the entire algorithm pseudocode. We also provide links to the python code in Appendix A. Next, we provide an empirical evaluation of the statistical robustness for the numerical constants we have selected for use in this paper.

B.1 Pseudocode for GP testbed

We describe the pseudocode for our testbed for any GP prior $N(\mu, \kappa)$ and any input distribution P_X . In our main experiments, we use the specific kernel $\mu = 0$, $\kappa = \kappa^1$ as outlined in Section 3.2.

- **Input:**

1. prior GP with mean function μ and kernel function κ
2. ENN f_θ
3. input distribution P_X and noise standard deviation σ
4. number of training data T and number of cached testing data T'
5. number of random indices M , and number of Monte-Carlo simulations N

- **Step 1 (generate training data and cache testing inputs):** sample T input data x_0, x_1, \dots, x_{T-1} i.i.d. from P_X ; also, sample T' cached testing data $x_T, x_{T+1}, \dots, x_{T+T'-1}$ i.i.d. from P_X . Let

$$\mathbf{x}_T = [x_0, \dots, x_{T-1}], \mathbf{x}_{T:T+T'} = [x_T, \dots, x_{T+T'-1}], \mathbf{x}_{T+T'} = [x_0, \dots, x_{T+T'-1}],$$

and sample a model $f^* \sim N(\mu, \kappa)$, restricted to $\mathbf{x}_{T:T+T'}$. Generate y_{t+1} for $t = 0, 1, \dots, T-1$ as

$$y_{t+1} = f_*(x_t) + \epsilon_{t+1},$$

where ϵ_{t+1} is independently sampled from $N(0, \sigma^2)$. Define the training dataset as $\mathcal{D}_T = \{(x_t, y_{t+1})\}_{t=0}^{T-1}$ and $\mathbf{y}_T = [y_1, \dots, y_T]$.

- **Step 2 (train ENN):** train ENN f_θ based on the training dataset \mathcal{D}_T . Let θ_T be the trained ENN parameters; that is, the trained ENN is f_{θ_T} .
- **Step 3 (GP inference):** based on the prior Gaussian process, the training data \mathcal{D}_T , and cached testing $\mathbf{x}_{T:T+T'}$, compute the Gaussian posterior over $f^*(\mathbf{x}_{T:T+T'}) \in \mathbb{R}^{T'}$. Assume that

$$\begin{aligned} \mu(\mathbf{x}_{T:T+T'}) &= \begin{bmatrix} \mu(\mathbf{x}_T) \\ \mu(\mathbf{x}_{T:T+T'}) \end{bmatrix} \\ \kappa(\mathbf{x}_{T:T+T'}) &= \begin{bmatrix} \kappa(\mathbf{x}_T) & \kappa(\mathbf{x}_T, \mathbf{x}_{T:T+T'}) \\ \kappa^T(\mathbf{x}_T, \mathbf{x}_{T:T+T'}) & \kappa(\mathbf{x}_{T:T+T'}) \end{bmatrix} \end{aligned}$$

Then, from Bayes' rule, we have

$$\begin{aligned} \mu(\mathbf{x}_{T:T+T'} | \mathcal{D}_T) &= \mu(\mathbf{x}_{T:T+T'}) + \kappa^T(\mathbf{x}_T, \mathbf{x}_{T:T+T'}) [\kappa(\mathbf{x}_T) + \sigma^2 I]^{-1} [\mathbf{y}_T - \mu(\mathbf{x}_T)] \\ \kappa(\mathbf{x}_{T:T+T'} | \mathcal{D}_T) &= \kappa(\mathbf{x}_{T:T+T'}) - \kappa^T(\mathbf{x}_T, \mathbf{x}_{T:T+T'}) [\kappa(\mathbf{x}_T) + \sigma^2 I]^{-1} \kappa(\mathbf{x}_T, \mathbf{x}_{T:T+T'}). \end{aligned}$$

To simplify the exposition, we define

$$\bar{\mu} = \mu(\mathbf{x}_{T:T+T'} | \mathcal{D}_T) \text{ and } \bar{\kappa} = \kappa(\mathbf{x}_{T:T+T'} | \mathcal{D}_T).$$

- **Step 4 (estimate KL-divergence):** For each $n = 1, \dots, N$: sample $x^{(n)}$ uniformly randomly from cached $\mathbf{x}_{T:T+T'}$. We use

$$\bar{\mu}^{(n)} = \bar{\mu}(x^{(n)}) \quad \text{and} \quad \bar{\kappa}^{(n)} = \bar{\kappa}(x^{(n)})$$

to respectively denote the posterior mean and variance at $x^{(n)}$. On the other hand, sample M i.i.d. indices $z_1^{(n)}, \dots, z_M^{(n)}$ from the epistemic reference distribution P_Z . Let $\hat{\mu}^{(n)}$ and $\hat{\kappa}^{(n)}$ denote the sample mean and sample variance of

$$f_{\theta_T}(x^{(n)}, z_1^{(n)}), f_{\theta_T}(x^{(n)}, z_2^{(n)}), \dots, f_{\theta_T}(x^{(n)}, z_M^{(n)}).$$

Finally, we estimate the KL as

$$\begin{aligned} \mathbb{E}[\mathbf{d}_{\text{KL}}(\mathbb{P}(f^*(X) \in \cdot | \mathcal{D}_T, X) \| \mathbb{P}(f_{\theta_T}(X, z \sim P_Z) \in \cdot | \theta_T, X)) | \mathcal{D}_T, \theta_T] \\ \approx \frac{1}{N} \sum_{n=1}^N \mathbf{d}_{\text{KL}} \left(\underbrace{N(\bar{\mu}^{(n)}, \bar{\kappa}^{(n)})}_{\text{true posterior}} \parallel \underbrace{N(\hat{\mu}^{(n)}, \hat{\kappa}^{(n)})}_{\text{ENN}} \right). \end{aligned}$$

The metric $\bar{\mathbf{d}}_{\text{KL}}$ can then be estimated by further averaging over training data \mathcal{D}_T and trained parameters θ_T . Section 3.2 outlines the sweep over settings and random seeds that we employ in our testbed.

B.2 Robustness of testbed

We now justify our choice of parameters N, T', M used in our experiments for Section 4. Following the pseudocode above, we motivate the quality of our KL estimate should improve as we sample larger N, T', M . However, we must balance this against the practical computational cost, and time, to run our experiments. Our goal therefore is to choose as small as feasible N, T', M so that our KL estimates of our agent evaluation is within some statistical margin of error.

For our testbed we selected $N = T' = 1000$ and $M = 100$. We arrived at these numbers through a combination of statistical intuition and computational running time in our code. To evaluate the robustness of these choices, we then vary these quantities as examine the estimates for our four ‘baseline’ agents in Section 4.1. Figure 9 shows the robustness to M , holding $N = T' = 1000$. We do see a trend that larger values of M tend to decrease the KL estimate, although by $M = 100$ these are all within 1 standard error and so we conclude that $M = 100$ is sufficient for our purposes. Figure 10 shows the robustness to $N = T'$, which set to be equal for simplicity, holding $M = 100$. The choice of $N = T'$ seems to make very little difference in our problem, on average, and so we simply set $N = T' = 1000$.

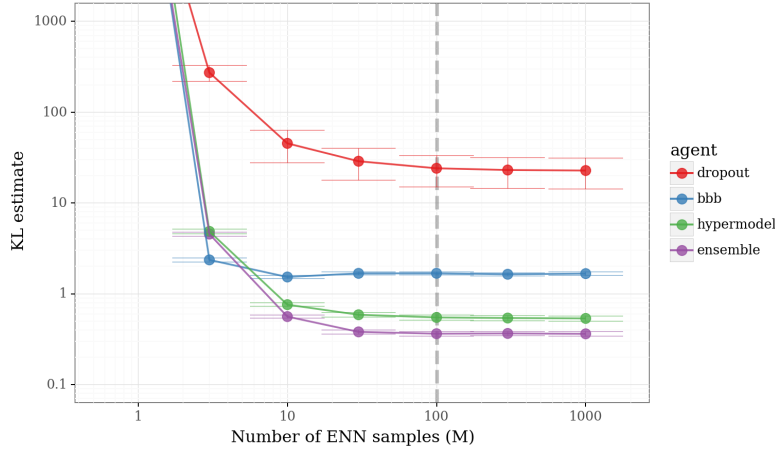


Figure 9: $M=100$ ENN samples is sufficient to give reasonable estimates of $\bar{\mathbf{d}}_{\text{KL}}$.

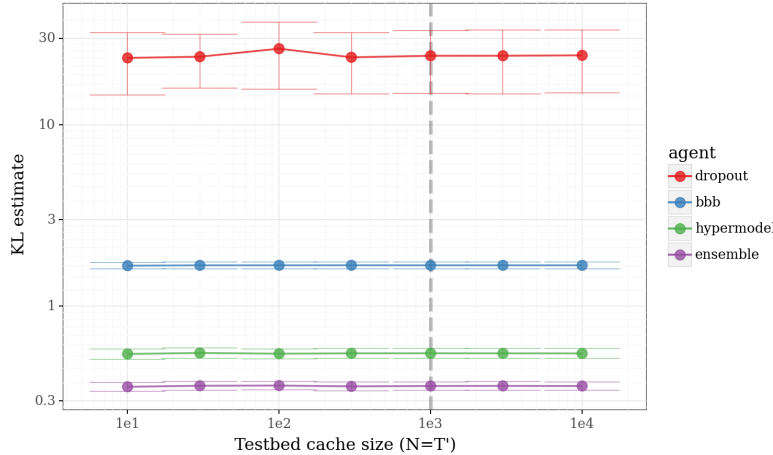


Figure 10: $N=T'=1000$ testing x points is sufficient to give reasonable estimates of $\bar{\mathbf{d}}_{\text{KL}}$.

C Choice of Testbed GP Kernel

We will specify our choice of the Gaussian process (GP) kernel in this section. In summary, let $D_{\mathcal{X}}$ denote the input dimension, we have chosen a kernel function $\kappa^1 : \mathbb{R}^{D_{\mathcal{X}}} \times \mathbb{R}^{D_{\mathcal{X}}} \rightarrow \mathbb{R}$ satisfying the following requirements:

- The GP $N(0, \kappa^1)$ corresponds to an infinitely wide neural network with zero-mean Gaussian weights and biases and the ReLU activation function.
- A sampled function $f \sim N(0, \kappa^1)$ tends to have complex patterns.
- The amount of data needed to learn the model scales reasonably with the input dimension $D_{\mathcal{X}}$.

We have chosen GPs corresponding to infinitely wide NNs due to its connection with deep learning problems. Also, this choice enables us to change the GP kernel with a few tuning knobs: the activation function, the number of hidden layers, and the weight and bias variances. In this section, we fix the activation function as the ReLU function and the number of hidden layers as two.

C.1 GP Corresponding to Infinitely Wide Neural Network

We first discuss how to recursively compute a kernel function κ s.t. the GP $f \sim N(0, \kappa)$ corresponds to an infinitely wide neural network with zero-mean Gaussian weights and biases. Our derivation in this subsection follows Lee et al. (2018). Consider the following neural network:

$$y_i^l(x) = b_i^l + \sum_{j=1}^{N_l} W_{ij}^l x_j^l(x) \quad \forall l = 0, 1, \dots, L \quad \text{and} \quad x_j^l(x) = \psi(y_j^{l-1}(x)) \quad \forall l = 1, \dots, L,$$

where l is the index for neural network layer, N_l is the number of nodes in layer l , i and j are indices for neural network node, and ψ is a nonlinear activation function (e.g. sigmoid, ReLU, and sign). Note that $x^0 = x$ is the input, and $y = y^L$ is the output, and $N_0 = D_{\mathcal{X}}$ is the input dimension.

Assume that b_i^l 's are drawn i.i.d. from $N(0, \sigma_{b,l}^2)$, and W_{ij}^l 's are drawn i.i.d. from $N(0, \sigma_{w,l}^2/N_l)$. Note that for any i , y_i^0 is a zero-mean GP, with kernel

$$\kappa^0(x, x') = \sigma_{b,0}^2 + \frac{\sigma_{w,0}^2}{N_x} \langle x, x' \rangle,$$

where $\langle x, x' \rangle$ is the inner product of x and x' . On the other hand, for each layer $l = 1, \dots, L$, as the number of nodes $N_l \rightarrow \infty$ (infinitely wide), from the central limit theorem, for any i , y_i^l is also a zero-mean GP, with kernel

$$\kappa^l(x, x') = \sigma_{b,l}^2 + \sigma_{w,l}^2 \mathbb{E}_{y^{l-1} \sim N(0, \kappa^{l-1})} [\psi(y^{l-1}(x)) \psi(y^{l-1}(x'))].$$

The above equation holds for any nonlinear function $\psi : \mathbb{R} \rightarrow \mathbb{R}$. For ReLU function, we have

$$\kappa^l(x, x') = \sigma_{b,l}^2 + \frac{\sigma_{w,l}^2}{2\pi} \sqrt{\kappa^{l-1}(x, x) \kappa^{l-1}(x', x')} \left(\sin \beta_{x,x'}^{l-1} + \left(\pi - \beta_{x,x'}^{l-1} \right) \cos \beta_{x,x'}^{l-1} \right),$$

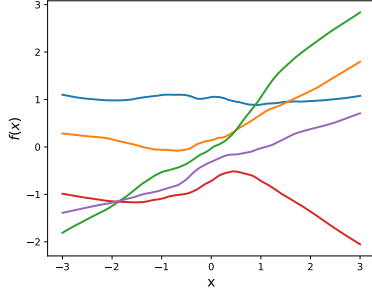
where

$$\beta_{x,x'}^{l-1} = \cos^{-1} \left(\frac{\kappa^{l-1}(x, x')}{\sqrt{\kappa^{l-1}(x, x) \kappa^{l-1}(x', x')}} \right).$$

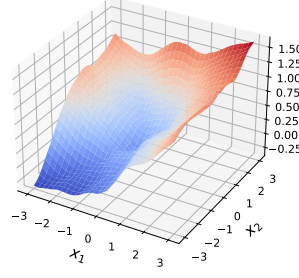
In this paper, we choose the GP kernel κ^1 as the one corresponding to the following infinitely wide NN with ReLU activation function:

- the number of hidden layers is $L = 2$.
- $\sigma_{w,l} = 1$ for $l = 0, 1, 2$; $\sigma_{b,0} = 1/\sqrt{D_{\mathcal{X}}}$, and $\sigma_{b,2} = \sigma_{b,1} = 0$.

First, we show that the sampled functions from $N(0, \kappa^1)$ tend to have complex patterns. Figure 11 plots some sampled functions from $N(0, \kappa^1)$ with input dimension $D_{\mathcal{X}} = 1, 2$, which indicates the sampled functions tend to have complex patterns.

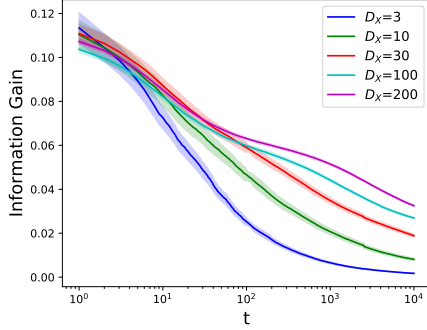


(a) $D_{\mathcal{X}} = 1$

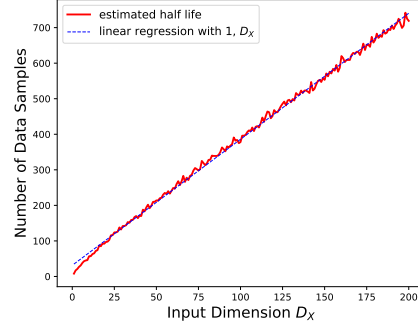


(b) $D_{\mathcal{X}} = 2$

Figure 11: Some randomly sampled functions from $N(0, \kappa^1)$ with $D_{\mathcal{X}} = 1, 2$.



(a) Information Gain



(b) Half Life

Figure 12: Information gain and half life under κ^1 with noise variance $\sigma^2 = 1$. The shaded region in the left figure indicates the standard deviation of the estimation.

C.2 Scalability with Input Dimension

In this subsection, we investigate the scalability of our chosen kernel κ^1 with respect to the input dimension $D_{\mathcal{X}}$. Our goal is to show that, the amount of data needed to learn the true model f^* scales reasonably with the input dimension $D_{\mathcal{X}}$. Consider the following process:

- **Step 1:** sample $f^* \sim N(0, \kappa^1)$
- **Step 2:** for each $t = 0, 1, \dots$, sample $x_t \sim N(0, I)$ and generate $y_{t+1} = f^*(x_t) + \epsilon_{t+1}$, where $\epsilon_{t+1} \sim N(0, \sigma^2)$.

Recall that $\mathcal{D}_t = \{(x_{t'}, y_{t'+1}) \text{ for } t' = 0, \dots, t-1\}$. Note that for the GP regression case, we can estimate the information gain $\mathbb{I}(f^*; y_{t+1} | \mathcal{D}_t, x_t)$ via Monte-Carlo simulation. For noise variance $\sigma^2 = 1$, the estimated $\mathbb{I}(f^*; Y_{t+1} | \mathcal{D}_t, X_t)$ as a function of number of training data t is plotted in Figure 12a for different input dimension $D_{\mathcal{X}}$. Note that the information gain decreases with the number of data t , and higher input dimension $D_{\mathcal{X}}$ requires more data to learn. In Figure 12b, we plot the “half life” of the information gain $\mathbb{I}(f^*; y_{t+1} | \mathcal{D}_t, x_t)$ as a function of the input dimension $D_{\mathcal{X}}$, which is defined as

$$\text{half_life} = \min\{t : \mathbb{I}(f^*; y_{t+1} | \mathcal{D}_t, x_t) \leq 0.5\mathbb{I}(f^*; y_1 | x_0)\}.$$

Figure 12b shows that the half life scales approximately linearly with the input dimension $D_{\mathcal{X}}$. This indicates that the amount of data needed to learn the true model f^* scales reasonably with the input dimension $D_{\mathcal{X}}$ under our chosen kernel κ^1 .